

Candidate High Redshift and Primeval Galaxies in Hubble Deep Field South

D.L. Clements¹, S.A. Eales¹, A.C. Baker¹

¹*Department of Physics and Astronomy, University of Wales Cardiff, PO Box 913, Cardiff, CF2 3YB*

18 April 2018

ABSTRACT

We present the results of colour selection of candidate high redshift galaxies in Hubble Deep Field South (HDF-S) using the Lyman dropout scheme. The HDF-S data we discuss were taken in a number of different filters extending from the near-UV (F300W) to the infrared (F222M) in two different fields. This allows us to select candidates with redshifts from $z \sim 3$ to $z \sim 12$. We find 15 candidate $z \sim 3$ objects (F300W dropouts), 1 candidate $z \sim 4$ object (F450W dropout) and 16 candidate $z \sim 5$ objects (F606W dropouts) in the ~ 4.7 arcmin² WFPC-2 field, 4 candidate $z \sim 6$ (optical dropouts) and 1 candidate $z \sim 8$ (F110W dropout) in the 0.84 arcmin² NICMOS-3 field. No F160W dropouts are found ($z \sim 12$). We compare our selection technique with existing data for HDF-North and discuss alternative interpretations of the objects. We conclude that there are a number of lower redshift interlopers in the selections, including one previously identified object (Treu et al., 1998), and reject those objects most likely to be foreground contaminants. Even after this we conclude that the F606W dropout list is likely to still contain substantial foreground contamination. The lack of candidate very high redshift UV-luminous galaxies supports earlier conclusions by Lanzetta et al. (1998). We discuss the morphologies and luminosity functions of the high redshift objects, and their cosmological implications.

Key words: galaxies;high-redshift – galaxies;formation – galaxies;interacting – galaxies;primeval

1 INTRODUCTION

Recent years have seen significant advances in our understanding of supposedly normal galaxies at high redshift ($z > 2$). This has been made possible by the introduction of simple photometric techniques that permit the successful selection of faint high redshift galaxies. These techniques include full-scale photometric redshift estimation methods (eg. Fernandez-Soto et al. (1998)), but perhaps the simplest is the Lyman-dropout method. This was pioneered by Steidel et al. (1995), and relies on the passage of the ubiquitous 912Å Lyman-limit discontinuity through broad-band imaging filters. At higher redshifts the suppression of light between 1216Å and 912Å in the emitted frame by the Lyman- α forest becomes significant, so that 1216Å becomes the break-point in the spectra (Spinrad et al. 1998). This approach was initially used with purpose built U,G and R filters (Steidel et al. 1995) to select galaxies at $z \sim 3$. The presence of the 912Å discontinuity in the U band leads to a large U-G colour while the flat spectral energy distribution redward of the Lyman break produces small G-R colours. The use of imaging filters allows large areas to be surveyed,

with the candidate high redshift galaxies later re-observed for spectroscopic confirmation. Several surveys have been conducted using this approach, and we are now able to probe the large scale distribution of $z \sim 3$ star-forming galaxies (eg. Steidel et al. (1998a)) and determine luminosity functions and colour distributions (eg. Dickinson et al. (1998)). It is also possible to extend this approach to higher redshifts by looking for the Lyman break at redder wavelengths (eg. Steidel et al. (1998b)).

Much of the work on high redshift galaxies in the original Hubble Deep Field (HDF-N) used the Lyman-break method to identify candidate objects (eg. Clements & Couch (1996), Madau et al. (1996)). The deep, high resolution imaging provided by HST allows selection of good candidates with lower luminosities than the ground-based Lyman-break galaxies, and permits studies of morphology that were previously very difficult. Application of the method redward of the bluest HDF-N filter, F300W, has also permitted the selection of candidate galaxies at $z \gg 3$, two of which have been spectroscopically confirmed at $z = 5.6$ (Weymann et al. 1998) and 5.34 (Spinrad et al., (1998)) and several others at $4 < z < 5$.

The main disadvantage of HDF-N, is its very small area on the sky. This means that the volume surveyed is a very small ‘pencil-beam’. When combined with the observed clustering of these objects (Steidel et al. 1998a), there may be significant problems in drawing any statistical conclusions (eg. Madau et al. (1996)) solely from HDF-N galaxies.

The HDF-South observations (HDF-S) thus offer us a significant potential increase in our knowledge of the high redshift universe. Apart from doubling the area surveyed with the Wide Field and Planetary Camera 2 (WFPC-2), the addition of the NICMOS infrared and STIS optical/UV observations allows us to significantly extend the redshift limits of the dropout technique. In principle, bright galaxies at $z > 12$ might even be detected as dropouts at $1.6\mu\text{m}$, appearing only in the longest wavelength band, $2.2\mu\text{m}$. The present paper applies simple Lyman-dropout selection techniques to the WFPC2 and NICMOS HDF-S data to provide initial lists of candidate galaxies out to the highest redshifts obtainable for use in further studies and in spectroscopic followup. We also discuss the implications of these results on our understanding of galaxy formation and the star formation history of the universe.

We use AB magnitudes throughout this paper and assume $H_0 = 50\text{kms}^{-1}\text{Mpc}^{-1}$, $q_0 = 0.5$ and $\Lambda = 0$.

2 SELECTION OF HIGH REDSHIFT CANDIDATES

The HDF-S data discussed here consists of observations from two separate regions. Firstly, the WFPC2 data, consisting of deep images in the F300W, F450W, F606W and F814W (3000\AA , 4500\AA , 6060\AA and 8140\AA respectively) filters reaching 10σ magnitude limits of 26.8, 27.7, 28.2 and 27.7 (in a 0.2 sq. arcsec. area) respectively (Williams et al. 1999) and covers an area of 4.7 sq. arcmin.. Secondly, the NICMOS Camera 3 region observed with the F110W, F160W, F222M filters ($1.1\mu\text{m}$, $1.6\mu\text{m}$ and $2.2\mu\text{m}$ respectively) and the STIS open CCD (STIS50) channel (covering 2000\AA to $1.1\mu\text{m}$) reaches 10σ magnitude limits of 27.0, 26.8, 24.0 and 28.4 (in 0.8 sq. arcsec. area) respectively and covers 0.84 arcmin^2 (Williams et al. 1999). Using the Lyman-break method we can thus, in principle, search for galaxies to redshifts > 12 using the F222M band.

To apply photometric selection criteria we must first extract photometric source catalogues for HDF-S. To achieve this we apply the SExtractor programme (Bertin & Arnouts 1996) to the combined drizzled images of the HDF-S provided by STScI (Williams et al. 1999). For WFPC2, objects are selected initially in the reddest filter, F814W, and then photometric parameters in other filters are measured at the positions of these objects. The objects are selected with a detection threshold of 1.5σ above the background and a minimum area of 0.4 arcseconds (ie. 10 connected pixels). This produces a total of 2257 detected objects. We use the ISO_MAG parameter extracted by SExtractor for source magnitudes, which gives the isophotal magnitude for an object down to 1.5σ above the background. This parameter is stable at faint limits and avoids any uncertainties resulting from correction to total magnitudes, though such corrections should amount to only $\sim 5\%$. This process pro-

duces a catalogue including magnitudes in all four passbands for each object detected in the F814W images.

For NICMOS, a somewhat different procedure is applied. Firstly, the STIS CCD image, which has a final pixel scale three times smaller than the drizzled NICMOS images, must be rebinned to match the NICMOS pixel scale to facilitate catalogue matching. Then, when searching for objects missing from filter a we select objects in filter b , the next reddest wavelength. Thus a catalog of objects missing from the STIS image, but detected at F110W, is based on a source list derived from the F110W filter, and similarly F110W dropouts are derived from a source list based on F160W detections. The SExtractor detection parameters are similar to those used for WFPC2. The F110W selected list contains 292 sources, the F160W list 342, and the F222M list 51, because of the lower magnitude limit due to the higher background in this filter.

Once the catalogues have been generated we select candidate high redshift objects using a technique derived from the extensive followup observations of HDF-N. Consideration of the colour-colour diagram for HDF-N galaxies in Dickinson (1998) shows that the following criteria will select the majority of high redshift objects in a given filter, a if:

- (i) The colour between the filter a and the next reddest filter $b > 1.5$
- (ii) The object should have been detected with at least 10σ significance in filter a if the colour $a - b = 1.5$
- (iii) There is no more than 1 magnitude difference between the flux in adjacent filters redder than b

Criterion 2 provides the magnitude limits for the present selection of candidate high z galaxies ie. $F450W < 25.3$ for F300W dropouts, $F606W < 26.2$ for F450W dropouts, $F814W < 26.7$ for F606W dropouts, $F110W < 26.9$ for STIS dropouts, $F160W < 25.5$ for F110W dropouts, and $F222M < 24$ for any F160W dropouts.

With these criteria we would select 9 of the 12 F300W dropout galaxies above our magnitude limit with spectroscopically confirmed redshifts in HDF-N (Dickinson 1998). We would also select all of the candidate $z > 4$ objects selected by photometric redshift methods above our magnitude limit, of which two have confirmed redshifts, given by Fernandez-Soto et al. (1998). Lower redshift interlopers are a potential problem. We can assess their contribution by examining the number of interlopers we would have selected in HDF-N. In Fernandez-Soto’s photometric and spectroscopic redshift compendium, we would select 17 F300W dropouts of which only 7 have either a spectroscopic or photometric redshift below 2. For F450W dropouts we would select just two objects, both at $z > 3.4$, while for F606W dropouts we would select 27 objects, of which only 5 lie at $z > 4.5$. Comparable data is not available in the infrared to test the NICMOS selections.

3 RESULTS

Using the above colour and magnitude criteria, we search our SExtractor catalogues for candidate high redshift galaxies from $z \sim 3$ to $z \sim 12$. The images of these candidate objects are then examined, leading to the rejection of several objects lying on the edge of, or beyond, the areas sur-

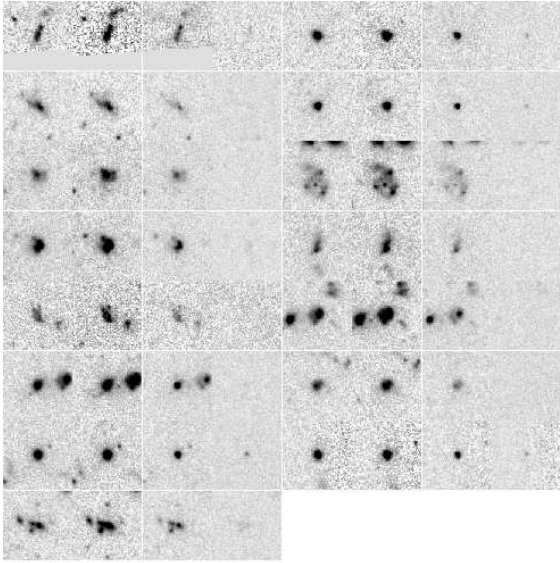


Figure 1. Images of F300W dropouts. Images are shown in groups of four horizontally, showing F814W, F606W, F450W and F300W images from left to right. Objects are shown in the same order as in Table 1, starting in the top left, then left to right, and then working down the page. Images are 4 arcseconds on a side. North is up and East is to the right.

veyed in one or more filters. The final catalogue of candidate high redshift objects is listed in Table 1. We find 15 possible F300W dropouts, candidate $z \sim 2.5$ – 3.5 objects, one $z \sim 3.5$ – 4.5 F450W dropout, 16 candidate F606W $z \sim 4.5$ – 5.5 dropouts, four candidate $z \sim 2.3$ – 7.0 STIS dropouts (though one, and possibly two, are lower redshift very red objects - see below). We find no candidate F110W or F160W dropouts within our magnitude limits, though we do find one fainter F110W dropout candidate which would lie at $z \sim 5.6$ – 9.7 . Images of the F300 dropout objects are shown in Figure 1.

4 DISCUSSION

4.1 High Redshift, Old or Red?

The determination of redshift estimates with broad band colours is a very inexact science, especially when limited to only a few passbands. The possibility exists that certain classes of lower redshift object might be able to mimic the colours of the dropout galaxies, and thus enter our list of candidate high redshift objects. Of specific concern are the Balmer decrement at 4000\AA in old galaxies, and the recently discovered highly dust obscured galaxies (Cimatti et al. 1998) known as Very Red Objects (Graham & Dey 1996).

The flux step across the 4000\AA break in ellipticals can be as high as a factor of 2 to 3 (eg. Coleman et al. (1980)). It is thus possible for old, red elliptical galaxies to masquerade as drop-outs at certain redshifts. For the F300W dropouts selection is based on the F300W-F450W colour so low redshift ellipticals might thus appear as F300W dropouts. Such objects would be bright, since they lie at lower redshift, and would have the distinctive $r^{1/4}$ surface brightness profile of an elliptical. Moderate redshift ellipticals could also inter-

fere with selection in other wavebands. For $z \sim 0.2$ – 0.5 they might appear as F450W dropouts, while at still higher redshift ($z \sim 0.5$ – 1) they could appear as F606W dropouts. The increasing volume encompassed by the HDF-S at higher redshifts will mean that an increasing number of foreground ellipticals will lie in the field for higher redshift selections. The problem of old, red objects is thus likely to be severest for the F606W dropouts, since there is ~ 3 – 4 times as much volume for foreground interlopers to appear through the 4000\AA break than for F450W dropouts.

The class of objects that has become known as Very Red Objects (VROs) also pose a problem. VROs are defined by their extremely red colours, $(R-K)_{\text{vega}} > 5$, or, equivalently, $(R-K)_{AB} > 3.3$. The nature of these objects is still unclear. They may simply be old ellipticals at large redshift, or they may be heavily dust-obscured objects containing either a starburst or an AGN (Egami et al., 1996). These objects could clearly appear in the NICMOS selected lists. Indeed, one VRO originally discussed by Treu et al. (1998) which is suggested to be an elliptical at $z > 1.7$, would appear to have been re-discovered by our selection as object no. 24, the brightest in our optical dropout selection (Treu et al., 1999). A further object, no. 255, seems likely to be a VRO, since it is also bright and significantly extended in the infrared — very similar to no. 24.

4.2 Absence of Very High Redshift Galaxies

HDF-S observations are capable of finding forming galaxies at very high redshifts – up to $z > 12$ for F160W dropouts. Galaxies forming stars at $100 (300) M_{\odot} \text{yr}^{-1}$ for $q_0 = 0.5(0.0)$ are detectable in the F222M filter. However, we find very few candidate very high redshift galaxies. Only one candidate $z \sim 8$ object is found, and no candidates at higher redshift. This supports the conclusions of Lanzetta et al. (1998) based on optical and near-IR observations of HDF-N that there are very few UV-luminous very high redshift galaxies. Combining the present results with those of Lanzetta et al., we conclude that the number density of these objects is $< 1.2 \text{ arcmin}^{-2}$. However, this limit refers only to *unobscured* very high redshift galaxies. Since these observations are dependent on detecting the far-UV emission from high redshift galaxies, even a moderate amount of obscuration could dim such objects below the detection threshold. The recent detection of a cosmological infrared background, eg. Puget et al. (1996), Fixsen et al. (1998), suggests that obscuration may have a significant role to play in the high redshift universe. We must thus treat these limits with caution.

4.3 Properties of Candidate High z Galaxies

The sizes of the candidate high redshift objects, as measured by the second moment of their F814 images for the WFPC2 objects and the F160W images for the NICMOS objects, range from a barely resolved $0.3''$, to $4.0''$. It is noticeable that the F300W dropouts are larger, with a mean size of $1.3'' \pm 0.3''$, compared to the more distant galaxies, with $0.72'' \pm 0.12''$ for the F606 dropouts. This does not necessarily reflect a cosmological effect. As noted above it is probable that there are more red, foreground elliptical galaxies contaminating the F606 dropouts. Such objects would have a

WFPC2 Cat. No.	RA(J2000)	Dec(J2000)	F814	F606	F450	F300
z~ 3 F300 Dropout Candidates						
38	22 32 53.98	-60 34 20.53	24.76±0.08	24.96±0.04	25.08±0.13	26.60±0.6
149 ¹	22 32 53.33	-60 34 13.69	22.83±0.02	23.21±0.01	23.88±0.04	26.14±0.26
257	22 32 59.91	-60 34 05.02	24.14±0.02	24.90±0.02	25.29±0.06	27.01±0.47
760 ¹	22 32 58.10	-60 33 37.08	23.13±0.01	23.60±0.01	24.29±0.03	26.28±0.29
877	22 33 04.89	-60 33 29.48	24.31±0.03	24.43±0.01	24.68±0.04	>27.8
880	22 32 50.64	-60 33 28.84	24.45±0.03	24.72±0.02	25.07±0.05	>27.8
895	22 33 03.19	-60 33 28.77	23.34±0.02	23.68±0.01	24.02±0.03	26.20±0.25
1158	22 33 03.87	-60 33 12.89	24.56±0.04	24.77±0.02	25.15±0.07	>26.6
1562	22 32 57.22	-60 32 41.50	24.55±0.04	24.78±0.02	25.03±0.07	27.00±0.69
1745	22 32 49.00	-60 32 26.85	23.44±0.02	23.61±0.01	24.14±0.03	>27.8
1748	22 32 49.22	-60 32 27.09	23.00±0.01	23.20±0.01	23.68±0.03	>26.9
1816	22 32 47.62	-60 32 20.61	24.43±0.03	24.84±0.02	25.26±0.06	>26.9
1847 ¹	22 32 47.76	-60 32 17.59	22.72±0.01	23.15±0.01	23.72±0.03	25.71±0.16
1934 ¹	22 32 46.51	-60 32 08.38	22.97±0.02	23.40±0.01	24.07±0.04	26.61±0.41
1951	22 32 48.87	-60 32 06.71	24.11±0.02	24.32±0.01	24.54±0.04	26.07±0.21
z~ 4 F450 Dropout Candidates						
1153	22 32 52.56	-60 33 15.47	24.70±0.03	25.62±0.02	27.27±0.17	>27.8
z~ 5 F606 Dropout Candidates						
17	22 32 59.66	-60 34 20.06	24.12±0.03	25.75±0.04	26.77±0.23	>26.25
50 ¹	22 33 00.58	-60 34 17.08	23.47±0.02	25.11±0.02	26.90±0.21	>27.5
211 ¹	22 32 57.79	-60 34 08.40	23.03±0.01	25.29±0.02	27.07±0.16	>27.8
494 ¹	22 32 55.39	-60 33 55.01	23.30±0.02	25.45±0.04	27.03±0.24	>26.6
601	22 33 05.11	-60 33 45.00	26.00±0.06	27.96±0.09	>28.7	>27.5
618	22 32 58.63	-60 33 46.22	25.83±0.05	27.51±0.07	>28.7	>27.8
836	22 33 00.00	-60 33 33.45	24.98±0.03	26.68±0.04	27.94±0.26	>27.8
872	22 32 56.80	-60 33 31.50	25.37±0.04	26.95±0.05	28.01±0.27	>27.3
899	22 32 57.07	-60 33 28.73	24.24±0.02	25.94±0.03	27.35±0.21	>27.8
1270	22 32 51.60	-60 33 06.55	24.38±0.03	26.14±0.04	27.67±0.26	>27.8
1364 ¹	22 32 57.98	-60 32 58.71	24.94±0.06	27.50±0.10	>28.7	>27.8
1473	22 32 57.96	-60 32 49.56	25.01±0.05	26.54±0.06	27.65±0.35	>26.5
1757	22 32 49.63	-60 32 27.64	26.58±0.08	28.40±0.10	>28.7	>27.8
2005	22 32 53.14	-60 32 01.58	24.81±0.03	26.66±0.04	>28.7	>27.0
2051	22 32 49.22	-60 31 58.69	26.35±0.07	28.00±0.08	>28.7	>27.8
2068 ¹	22 32 55.94	-60 31 56.49	24.43±0.03	26.81±0.05	28.33±0.35	>27.8
NICMOS Cat. No.	RA(J2000)	Dec(J2000)	F222	F160	F110	STIS
z~ 6 Optical Dropout Candidates						
24*	22 32 51.09	-60 39 09.80	21.29±0.08	21.79±0.01	22.72±0.02	25.93±0.25
99	22 32 55.20	-60 38 52.19	23.9±0.50	24.16±0.03	24.32±0.04	26.57±0.25
110	22 32 49.10	-60 38 50.75	>24.0	27.03±0.07	26.82±0.08	29.07±1.00
255 ²	22 32 51.22	-60 38 22.56	23.04±0.16	23.70±0.01	24.64±0.02	26.74±0.25
z~ 8 F110 Dropout Candidates						
189	22 32 48.27	-60 38 43.69	24.9±0.50	26.36±0.07	>28.0	28.3±0.70
z~ 12 F160 Dropout Candidates						

None

Table 1. Details of drop out galaxies

Limits are 3σ upper limits. ¹ indicates likely low redshift interloper, * Treu et al. (1998) VRO at $z>1.7$. ² indicates other possible low z VRO. See text for details.

smaller size than the often very extended and disturbed genuine high redshift galaxies. In this context it is interesting to note that the smallest F300 dropout objects are often the brightest eg. objects 149 and 1847. A similar effect can also be noted in the F606 dropouts. These objects are also those which most often have some faint emission in the dropout band, which tends to corroborate the suggestion that they are lower redshift interlopers. We thus suspect that several of the smaller brighter objects may be foreground interlopers. These are noted in Table 1. A more stringent selection criterion for F606 dropouts using $F814 - F606 > 2.0$ instead of 1.5 would select just three objects in HDF-N, all of which have spectroscopic or photometric redshifts > 4.5 . For HDF-S this selection produces no believable high redshift candidates. On the basis of this and the number of interlopers the selection would select in HDF-N, the F606W dropout list should probably be treated with caution until spectroscopic redshift confirmations are available.

The morphologies of the candidate high redshift galaxies show an interesting shift from F300 dropouts to longer wavelength selections. Many of the F300 dropouts show disturbed extended morphologies, as is the case for similar objects in HDF-N (Clements & Couch 1996). These include the spectacularly disturbed object 880, and an apparent interacting pair of dropout galaxies 1745 and 1748, which may be a similar system to the famous ‘Hotdog’ galaxy in HDF-N (Bunker et al. 1998). In contrast, most of the longer wavelength dropout candidates are smaller and with much less unusual morphologies. This might indicate that the higher redshift objects are the original pre-galactic clumps which then merge together at around $z \sim 3$ to form larger objects, or alternatively might just be due to the cosmological $(1+z)^4$ surface brightness dimming from $z \sim 3$ to $z \sim 5$ and above.

Figure 2 shows a comparison of the UV ($\sim 1600\text{\AA}$) luminosity function (LF) of $2.5 < z < 3.5$ galaxies in Fernandez-Soto et al. (1998), all of which have spectroscopic confirmation, with the LF of F300 dropout galaxies from the present paper, after the removal of the small, bright galaxies discussed above. As can be seen the LFs match very well.

5 CONCLUSIONS

We have selected candidate high redshift galaxies using the established Lyman ‘drop-out’ technique, but have applied this to the widest range of wavelengths possible in the HDF-S. We have found candidate galaxies up to $z \sim 8$. A number of the dropout selected objects, though, are identified as low redshift interlopers, demonstrating the need for spectroscopic followup and observations over a broader wavelength range. We note that the $z \sim 3$ F300W selected objects typically show highly disturbed morphologies while candidates at higher redshifts do not, perhaps indicating that $z \sim 3$ saw the onset of substantial galaxy or galaxy-subunit merging. We will next develop more sophisticated photometric redshift modelling and will apply this to broader wavelength observations of HDF-S as they become available.

Acknowledgements It is a pleasure to thank the HDF and HDF-S teams at STScI and STECF and E. Bertin for SExtractor. The anonymous referee made many useful comments that have improved the paper. DLC and ACB are supported by PPARC postdoc grants.

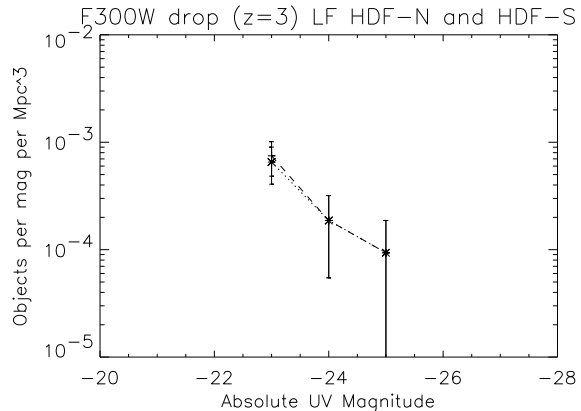


Figure 2. $z=3$ Lyman Dropout Galaxy Luminosity Function

Comparison of the HDF-N and HDF-S $z \sim 3$ Lyman dropout galaxy luminosity functions. Data for HDF-N from (Fernandez-Soto et al. 1998) data for HDF-S from the present paper, excluding four bright, small objects. HDF-N LF is shown by the dotted line, HDF-S uses a dashed line. Note the good match between the two data sets.

REFERENCES

- Bertin, E., Arnouts, S., 1996, *A&AS*, 117, 393
 Bunker, A.J., Stern, D., Spinrad, H., Dey, A., Steidel, C.C., 1998, *BAAS*, 192, 7008
 Cimitti, A., Andreani, P., Rottgering, H., Tilanus, R., 1998, *Nature*, 392, 895
 Clements, D.L., Couch, W.J., 1996, *MNRAS*, 280, L43
 Coleman, G.D., Wu, C.-C., Weedman, D.W., 1980, *ApJS*, 43, 393
 Dickinson, M., Proceedings of the STScI Symposium ‘The Hubble Deep Field’, ed. Livio, M., Fall, S.M., Madau, P., in press, astro-ph/9802064
 Egami, E., Iwamuro, F., Maihara, T., Oya, S., Cowie, L.L., 1996, *AJ*, 112, 73
 Fernandez-Soto, A., Lanzetta, K., Yahil, A., 1998, *ApJ* submitted, astro-ph/9809126
 Fixsen, D.J., Dwek, E., Mather, J.C., Bennett, C.L., Shafer, R.A., 1998, *ApJ*, 508, 123
 Graham, J.R., Dey, A., 1996, *ApJ*, 471, 720
 Lanzetta, K.M., Yahil, A., Fernandez-Soto, A., 1998, *AJ*, 116, 1066
 Madau, P., Ferguson, H.C., Dickinson, M.E., Giavalisco, M., Steidel, C.C., Fruchter, A., 1996, *MNRAS*, 283, 1388
 Puget, J.-L., Abergel, A., Bernard, J.-P., Boulanger, F., Burton, W.B., Desert, F.-X., Hartmann, D., 1996, *A&A*, 308, L5
 Spinrad, H., Stern, D., Bunker, A., Dey, A., Lanzetta, K., Yahil, A., Pascarelle, S., Fernandez-Soto, A., 1998, *AJ*, 116, 2617
 Steidel, C.C., Pettini, M., Hamilton, D., 1995, *AJ*, 110, 2519
 Steidel, C.C., Adelberger, K.L., Dickinson, M., Giavalisco, M., Pettini, M., Kellogg, M., 1998, *ApJ*, 492, 428
 Steidel, C.C., Adelberger, K.L., Dickinson, M., Giavalisco, M., Pettini, M., 1998, in Proceedings of the Xth Rencontres de Blois, ‘The Birth of Galaxies’, astro-ph/9812167
 Treu et al., 1998, *A&A*, 340, L10
 Treu et al., 1999, *A&A*, in press
 Weymann, R.J., Stern, D., Bunker, A., Spinrad, H., Chaffee, F.H., Thompson, R.I., Storrie-Lombardi, L.J., astro-ph/9807208
 Williams, R., et al., *AJ*, in press and STScI webpages